REPORT

Recessive Mutations in *RTN4IP1* Cause Isolated and Syndromic Optic Neuropathies

Claire Angebault,[1,12] Pierre-Olivier Guichet,[1,12] Yasmina Talmat-Amar,[1,12] Majida Charif,[1,2,13]
Sylvie Gerber,[3,13] Lucas Fares-Taie,[3,13] Naig Gueguen,[2] François Halloy,[1] David Moore,[4]
Patrizia Amati-Bonneau,[2] Gael Manes,[1] Maxime Hebrard,[1] Béatrice Bocquet,[5] Mélanie Quiles,[1]
Camille Piro-Mégy,[1] Marisa Teigell,[1] Cécile Delettre,[1] Mireille Rossel,[6] Isabelle Meunier,[1,5]
Markus Preising,[7] Birgit Lorenz,[7] Valerio Carelli,[8,9] Patrick F. Chinnery,[4] Patrick Yu-Wai-Man,[4,10]
Josseline Kaplan,[3] Agathe Roubertie,[1,5] Abdelhamid Barakat,[11] Dominique Bonneau,[2] Pascal Reynier,[2]
Jean-Michel Rozet,[3] Pascale Bomont,[1] Christian P. Hamel,[1,5] and Guy Lenaers[1,2,*]

Autosomal-recessive optic neuropathies are rare blinding conditions related to retinal ganglion cell (RGC) and optic-nerve degeneration, for which only mutations in *TMEM126A* and *ACO2* are known. In four families with early-onset recessive optic neuropathy, we identified mutations in *RTN4IP1*, which encodes a mitochondrial ubiquinol oxydo-reductase. RTN4IP1 is a partner of RTN4 (also known as NOGO), and its ortholog Rad8 in *C. elegans* is involved in UV light response. Analysis of fibroblasts from affected individuals with a *RTN4IP1* mutation showed loss of the altered protein, a deficit of mitochondrial respiratory complex I and IV activities, and increased susceptibility to UV light. Silencing of *RTN4IP1* altered the number and morphogenesis of mouse RGC dendrites in vitro and the eye size, neuro-retinal development, and swimming behavior in zebrafish in vivo. Altogether, these data point to a pathophysiological mechanism responsible for RGC early degeneration and optic neuropathy and linking *RTN4IP1* functions to mitochondrial physiology, response to UV light, and dendrite growth during eye maturation.

Inherited optic neuropathies (IONs) are neurodegenerative diseases affecting the visual pathway and are frequently associated with extra-ocular symptoms.[1,2] Dominant IONs (dominant optic atrophy [DOA] [MIM: 165500]) are mostly caused by mutations in *OPA1*[3,4] (MIM: 605290) and rarely by mutations in *OPA3*[5] (MIM: 606580); both genes encode inner mitochondrial proteins. Non- or pauci-syndromic recessive IONs occur less frequently, and several families affected by these recessive forms have recently been linked to *TMEM126A* (MIM: 612988) and *ACO2*[6,7] (MIM: 100850) mutations.

Informed consent was obtained from all patients for clinical examination and genetic analysis, according to approved protocols of the Montpellier University Hospitals and in agreement with the Declaration of Helsinki. The Ministry of Public Health approved the biomedical research under the authorization number 11018S. In a consanguineous Moroccan family affected by an autosomal-recessive ION, we performed SNP genotyping (GeneChip Human Mapping 250K SNP Array, Affymetrix) in the proband (I-3, Figure 1A) and identified four homozygous regions on chromosomes 1, 6, 18, and 22 of 12.2,

19, 22.6, and 23.4 megabases, respectively. After exome sequencing (SureSelectXT Human All Exon V5 [Agilent] followed by Illumina HiSeq2000) and filtering for rare (<1/300) homozygous variants present in genes that are included in these regions and that encode for mitochondrial proteins, we identified a c.308G>A (p.Arg103His) substitution in *RTN4IP1* (MIM: 610502) (GenBank: NM_032730.4), encoding the RTN4-interacting protein 1,[8] in the 19 Mb homozygous region of chromosome 6 (Figure 1B). This change was referenced in the NCBI database (rs372054380 [GenBank: NP_116119.2]) and had a heterozygous frequency of 2/13,004 in the NHLBI Exome Sequencing Project Exome Variant Server and 1/121,304 in the ExAC Browser databases. It modifies an amino acid evolutionarily conserved among vertebrates (Figure 1C) and is predicted to be functionally damaging (scores of 0.01 and 1 via SIFT and PolyPhen-2, respectively). Both affected individuals from this family were homozygous for the missense mutation, whereas their parents and three unaffected relatives, II-1, II-2, and II-6, were heterozygous. Affected siblings II-3 and II-4 had presented with low vision since early childhood and did not complain of any

[1]INSERM U1051, Institut des Neurosciences de Montpellier, Université de Montpellier, 34090 Montpellier, France; [2]INSERM U1083, CNRS 6214, Département de Biochimie et Génétique, Université LUNAM and Centre Hospitalier Universitaire, 49933 Angers, France; [3]INSERM U1163, Hôpital Necker Enfants-Malades, 75015 Paris, France; [4]Institute of Genetic Medicine, Centre for Life, Newcastle University and Wellcome Trust Centre for Mitochondrial Research, NE1 3BZ Newcastle upon Tyne, UK; [5]Centre de Référence pour les Maladies Sensorielles Génétiques, Hôpital Gui de Chauliac, CHRU Montpellier, 34090 Montpellier, France; [6]INSERM U710, Laboratoire MMDN EPHE, 34090 Montpellier, France; [7]Department of Ophthalmology, Justus-Liebig University, 35392 Giessen, Germany; [8]IRCCS, Institute of Neurological Sciences of Bologna, Bellaria Hospital, 40139 Bologna, Italy; [9]Department of Biomedical and NeuroMotor Sciences, University of Bologna, 40139 Bologna, Italy; [10]Newcastle Eye Centre, Royal Victoria Infirmary, NE1 4LP Newcastle upon Tyne, UK; [11]Laboratoire de Génétique Moléculaire Humaine, Département de Recherche Scientifique, Institut Pasteur du Maroc, 20360 Casablanca, Morocco
[12]These authors contributed equally to this work
[13]These authors contributed equally to this work
*Correspondence: guy.lenaers@inserm.fr
http://dx.doi.org/10.1016/j.ajhg.2015.09.012. ©2015 by The American Society of Human Genetics. All rights reserved.
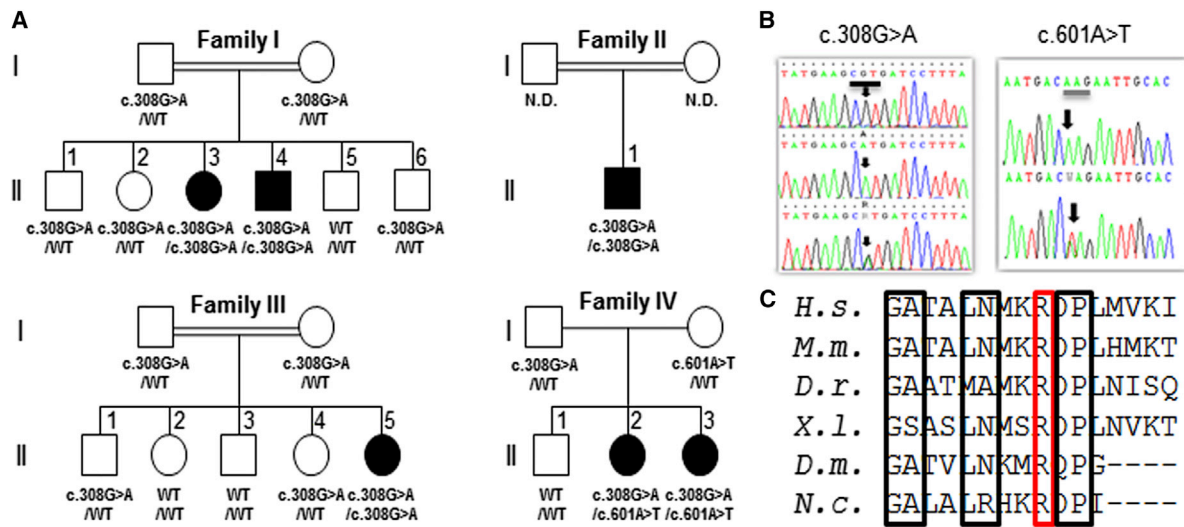
Figure 1. Identification of *RTN4IP1* Mutations in Four Families

(A) Family pedigrees showing the affected members in black and the segregation of the c.308G>A and c.601A>T mutations. N.D., no genetic diagnosis.

(B) Electrophoregram presenting the *RTN4IP1* c.308G>A (left) and c.601A>T (right) mutations.

(C) RTN4IP1 ortholog protein sequence alignment showing the evolutionarily conserved positions around arginine 103, which is squared in red. Informed consent was obtained from all individuals to perform genetic and biochemical analysis. *H.s.*, *Homo sapiens*; *M.m.*, *Mus musculus*; *D.r.*, *Danio rerio*; *X.l.*, *Xenopus laevis*; *D.m.*, *Drosophila melanogaster*; *N.c.*, *Neurospora crassa*.

other symptoms (Table S1). Fundus examination revealed moderate bilateral optic-disk pallor (Figure 2A), and optical coherence tomography disclosed a marked decrease in the thickness of the retinal nerve fiber layer in the temporal side (Figure 2B), a characteristic feature of mitochondrial forms of hereditary optic atrophy.

Screening of *RTN4IP1* by Sanger sequencing in a cohort of 240 European ION-affected probands without genetic diagnosis identified four additional affected subjects. Two of them were simplex-case subjects of Roma origin (families II and III, Figure 1A) who were also homozygous for the c.308G>A (p.Arg103His) substitution on the same haplotype, suggesting a founder effect (Figure S1). The

affected individuals had mild to moderate optic atrophy similar to the individuals of family I and showed no additional symptoms (Table S1). The two other additional subjects (IV-2 and IV-3, Figure 1A) were sisters from a multiplex family carrying compound heterozygous mutations, including the c.308G>A variant found in families I, II, and III but on a different haplotype (Figure S1) and a nonsense c.601A>T (p.Lys201*) variant (Figure 1B) leading to the truncation of the last 196 amino acids of the protein. This latter mutation was not referenced in databases. The parents were heterozygous for one of each mutated allele, and the unaffected brother carried no mutation. The two sisters presented similarly in early life, with a severe
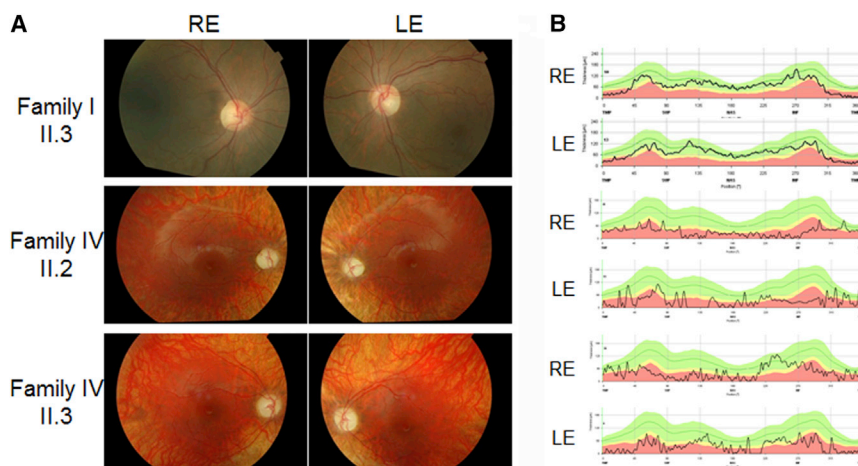

Figure 2. Ophthalmological Exploration of Individuals Affected by *RTN4IP1* Mutations

(A) Fundus examinations (RE, right eye; LE, left eye) of the individuals I-3 from family I (top) and IV-2 (middle) and IV-3 (bottom) from family IV revealed temporal pallor of the optic discs and a peripheral de-pigmented retina for the two sisters of family IV.

(B) Optical coherence tomography scanning and measurement of the retinal nerve fiber layer of the optic disks showed a drastic reduction in thickness (black line) in the temporal quadrants of individual I.3 from family I (top) and in all the quadrants of the two sisters in family IV (middle and bottom). The green area corresponds to the 5th to 95th percentile, the yellow area corresponds to the 1st to 5th percentile, and the red area corresponds to below the 1st percentile. RE, right eye; LE, left eye.
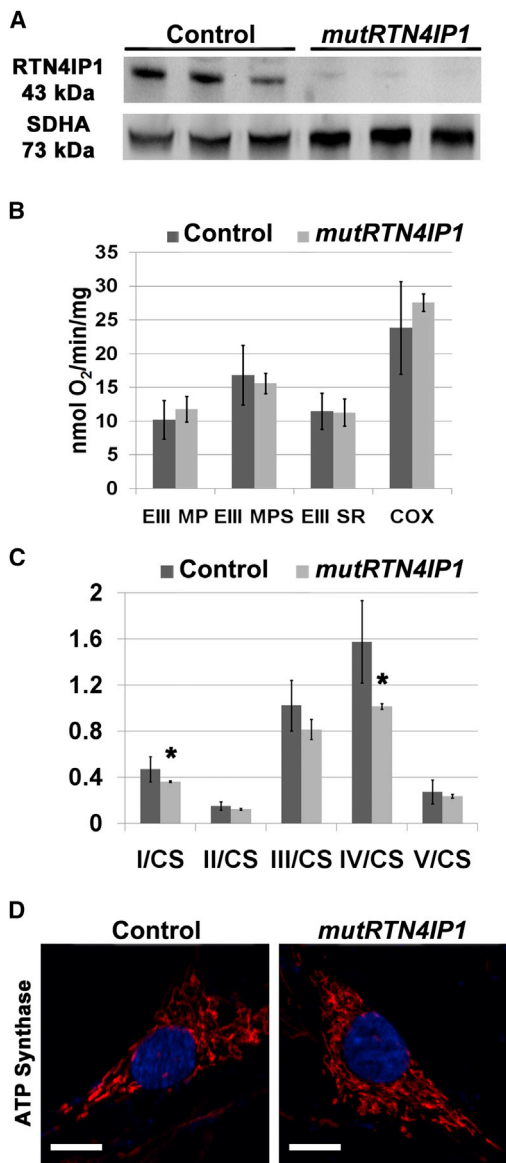
Figure 3. Molecular and Cellular Characterization of *RTN4IP1* Mutated Fibroblasts

(A) Western blot against RTN4IP1 (top; Abcam antibodies 1/1,000) and SDHA (bottom; Abcam antibodies 1/1,000) on purified mitochondrial extracts from three control fibroblast strains and from the fibroblasts from the index case subject (I-3) in family I and from the two sisters (IV-2 and IV-3) in family IV shows the drastic reduction of RTN4IP1 abundance in mutated cells.

(B) Assessment of the mean oxygen consumption from the three control and the three *RTN4IP1* mutated fibroblast strains related to complexes I (EIIIMP), I + II (EIIIMPS), II (EIIISR), and IV (COX), measured with a high-resolution Oxygraph respirometer and Oroboros protocols, did not reveal a significant difference between control and mutated fibroblasts.

(C) Mean enzymatic activities of the respiratory complexes (CI to CV) from the three control and the three *RTN4IP1* mutated fibroblast strains related to the citrate synthase (CS) enzymatic activity were assayed by standard procedures[23–25] and revealed a significant reduction of complex I and complex IV activities in mutated fibroblasts.

(D) The structure of the mitochondrial network is not affected in *RTN4IP1* mutated fibroblasts as compared to that in wild-type fibroblasts, as assessed by ATP synthase immunofluorescence. Scale bar represents 10 μm.

bilateral optic neuropathy, associated with nystagmus, a mild stato-kinetic cerebellar syndrome, and learning disabilities. The older sister was more severely affected with mild mental retardation and exhibited generalized seizures from the age of 3 years (Table S1). Fundus examinations of both sisters disclosed abnormal optic disks, which appeared small with a horizontal orientation and were pale on their entire surface (Figure 2A), possibly reflecting a subtle hypoplasia. The thickness of the retinal nerve fiber layer was dramatically reduced in all quadrants (Figure 2B). There was no detectable visual evoked potential, and the optic tracts were thin in brain MRI, indicative of the severe alteration of the optic path. The brain was otherwise normal, as were the cerebral spectroscopic MRI, ENT, cardiologic, and neuro-muscular examinations (Table S1).

To gain insight into the pathophysiological mechanisms, we studied skin-derived fibroblasts from the proband of family I and from the two affected sisters of family IV. Assessment of *RTN4IP1* expression revealed that the mRNA abundance remained unaffected (data not shown), whereas that of the altered protein was drastically reduced (>95%, Figure 3A) and that of the truncated protein was undetectable. Because *RTN4IP1* encodes a mitochondrial protein,[8] we monitored respiratory parameters. Oxygen consumptions driven by complex CI, CI + CII, CII, and CIV were normal in mutated fibroblasts (Figure 3B), whereas enzymatic activities of CI and CIV were significantly reduced in *RTN4IP1* fibroblasts (Figure 3C). We further analyzed the structure of the mitochondrial network and did not find evidence of significant fusion or fission defect (Figure 3D), nor did we find a difference in mtDNA copy number (data not shown) between wild-type and *RTN4IP1* mutated fibroblasts. Because the *Caenorhabditis elegans* ortholog of *RTN4IP1* is *Rad8*, a gene involved in UV light sensitivity,[9,10] we monitored the susceptibility to UV light of fibroblasts. Exposure of *RTN4IP1* mutated fibroblasts to UV light induced a straight cell morphological change, with altered fibroblasts adopting a round shape in less than 30 min (Figure S3A) and tending to detach from the support. After overnight incubation, we found a 2-fold increase in apoptosis in mutated cells compared to that in control cells (Figure S3B), a finding consistent with RTN4IP1's involvement in the response to UV light exposure.[11]

We then assessed whether RTN4IP1 subcellular localization is consistent with its predicted N-terminal 41-amino-acid-long mitochondrial targeting peptide[8] and its known interaction with RTN4 (also known as NOGO) (MIM: 604475) at the ER.[12] The RTN4IP1-EYFP fusion protein colocalized with the mitochondrial ATPase protein (Figure S2A) and partially colocalized with the GRP78 protein from the ER at spots corresponding to contact
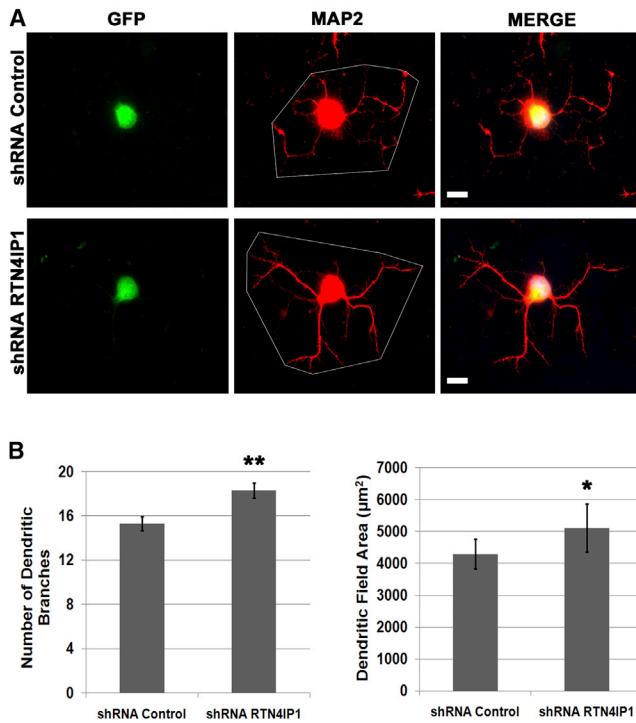
Figure 4. Altered Dendritogenesis in Retinal Ganglion Cells Depleted for *Rtn4ip1*

RGCs were obtained from the retinas of 3-day-old mouse pups with the CELLection Pan Mouse IgG Kit (Invitrogen) and the Anti-CD90 antibody (AbD Serotec). GIPZ Lentiviral Mouse *Rtn4ip1* shRNA and GIPZ Lentiviral Mouse Non-Silencing shRNA (control) were obtained from Thermoscientific. For RGC transduction, cells were seeded at 5×10^4 cells in 96-well plates with poly-D-lysine- and laminin-coated glass coverslips and infected at an multiplicity of infection of five. 4 days later, cells were processed for immunofluorescence analyses. Efficiency of shRNA silencing was assessed on NIH 3T3 cells and showed a 60% reduction of *Rtn4ip1* mRNA abundance.

(A) Expression of the control (top) and the *Rtn4ip1* mouse-specific (bottom) shRNA in RGCs processed for immunofluorescence with Map2 (Abcam, 1/5,000 antibodies). Fluorescent pictures show the nuclear GFP labeling (left) and the Map2 labeling (middle) and their superposition (MERGE; right), revealing the dendritic arborization of the infected GFP-positive neurons.

(B) Quantification of dendritic arborization reveals significant increases in the number of branches (top) and the total dendritic area (polygon obtained by joining the distal extremities of each dendrite; bottom) in cells transfected with the lentivirus expressing the *Rtn4ip1* versus the control shRNA. Data are representative of three independent experiments. 120 cells were analyzed for each condition. Results are given as mean $\pm$ SEM. Stars indicate significant Mann-Whitney tests: *$p < 0.05$; **$p < 0.01$. Scale bar represents 10 μm.

sites with mitochondria (Figure S2B). Mitochondrial sublocalization study, using increasing concentrations of digitonin and proteinase K digestion, suggested that, together with BCL2, RTN4IP1 is associated with the outer membrane (Figure S3C), thus supporting the possibility of cross-talk between RTN4IP1 at the surface of mitochondria and RTN4 from the ER. Because RTN4 regulates dendrite branching and extension during development of the CNS,[13–15] we assessed the effects of *Rtn4ip1* silencing

on RGC arborization. Depletion of Rtn4ip1 in RGCs from mouse pups, via lentivirus-targeted shRNA, revealed a significant increase in dendrite numbers (+19%, ± 4.55%) and in total surface area of dendritic arborization (+20%, ± 17.5%) (Figures 4A and 4B), suggesting that Rtn4ip1 acts as a regulator of Rtn4 function and controls RGC neurite outgrowth. Finally, we addressed whether *RTN4IP1* invalidation could reproduce in vivo the clinical phenotype seen in affected individuals. For this purpose, we silenced the expression of its zebrafish ortholog, which has 67% identity with and 91% similarity to its human counterpart, by using antisense morpholino oligonucleotides. Injection in fertilized eggs of a morpholino targeting exon 2 splicing (MO) and of a control mismatch morpholino (MI) did not affect the overall development at 24 hr post fertilization (hpf). However, in MO-injected animals, a detectable alteration in the morphology of the eyes was noticeable from 48 hpf onward, becoming severely abnormal at 72 hpf; MO morphants caused a significant reduction in ocular size (Figure 5A). This correlated with a drastic absence of RGC and plexiform layers in retinal histological slices from *rtn4ip1*-silenced fish (Figure 5B), which exhibited a looping swimming behavior typical of visually impaired fish (Figure 5C and Movies S1, S2, and S3).Together, both the deep structural alterations of the retina with early RGC degeneration and the functional visual impairment[16,17] evidenced in *rtn4ip1*-silenced zebrafish parallel the ophthalmological observations in individuals with *RTN4IP1* mutations.

In conclusion, we identified mutations in *RTN4IP1* that, like mutations in *TMEM126A* and *ACO2*, induce an early-onset optic neuropathy that might be followed by the development of additional neurological symptoms. These three genes encode mitochondrial proteins with divergent functions in mitochondria,[6,7] but none of them is involved in mitochondrial dynamics, in contrast to the proteins encoded by genes mutated in dominant optic neuropathies, namely *OPA1* and *OPA3*. Nevertheless, the decrease in CI and CIV enzymatic activities in individuals with *RTN4IP1* mutations recapitulates the mitochondrial respiratory chain dysfunctions observed both in DOA and Leber hereditary optic neuropathy. However, in contrast to these diseases, the very early onset of visual dysfunction in persons harboring *RTN4IP1* mutations suggests an impairment of RGC maturation or even a developmental alteration of the inner retina and optic nerve. Indeed, in the individuals who harbor the presumably most severe alteration (p.Lys201*), we found that the optic discs were of smaller size and had a horizontal tilt, suggesting that the content in fibers was already decreased when the optic nerves were formed at a prenatal stage. The observation of small eyes totally lacking retinal ganglion cells and inner retinal layers in *rtn4ip1*-silenced zebrafish larvae is in line with the human findings and with an abnormal development of the retinal ganglion cells. This could plausibly be related to the lack of interaction between RTN4IP1 and the RTN4 pathway,[12,18] which would have a negative
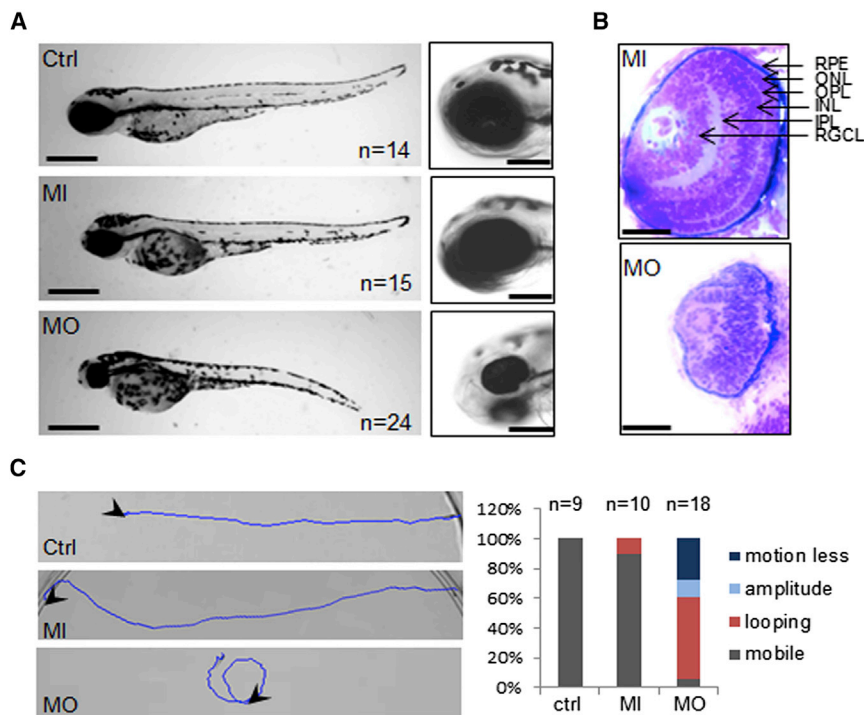
Figure 5. Phenotype Associated with the Silencing of the *RTN4IP1* Ortholog in Zebrafish

Zebrafish (*Danio rerio*) of the AB genetic background were maintained at 28°C on a 14-hr-light and 10-hr-dark cycle. Eggs were injected with antisense *rtn4ip1* morpholino nucleotides (MO) and mismatch nucleotides (MI) at a concentration of 0.3 pM and monitored up to 72 hpf. They produced reproducible phenotypes. The *rtn4ip1* MO morpholino (Gene Tools) was designed against the splice junction between intron 1 and exon 2. Sequences are *rtn4ip1* MO: 5′-ATAGCCACCTACAAGAG CGAAAATA-3′ and control MI: 5′-ATACC GACCTAGAAGACCCAAAATA-3′.

(A) To observe global larvae morphology, we imaged whole-mount animals with a Zeiss SteREO Discovery V20 microscope and their heads with by a Zeiss AxioImager.D2 microscope. Representative phenotypes of 72-hr-old control larvae (Ctrl; top) and larvae derived from fertilized eggs injected with a mismatch (MI; middle) or *rtn4ip1*-specific (MO; bottom) morpholino. Depletion of rtn4ip1 does not show developmental modification (left; scale bar represents 500 μm), except for the size of the eye (right; scale bar represents 250 μm); the ocular diameter is clearly reduced in larvae treated with the *rtn4ip1* morphant.

(B) Histological analysis of the eye was done on larvae fixed in 2.5% glutaraldehyde and 4% paraformaldehyde overnight and post-fixed in 1% osmotic acid + 0.8 potassium ferrocianide for 2 hr in the dark and at room temperature. After two washes in Sorensen's buffer, tissues were dehydrated in a graded series of ethanol solutions (30%–100%) and then embedded in EmBed 812 with a Leica EM AMW Automated Microwave Tissue Processor for Electronic Microscopy.[26] Semi-thin sections of retina (1 μm) were collected, stained with toluidine bleu, and imaged by a Zeiss AxioImager D2 microscope. Normal retinal structure in larvae derived from eggs injected with the mismatch morpholino (MI; top) showed the retinal pigmentary epithelium (RPE), the outer nuclear layer (ONL), the outer plexiform layer (OPL), the inner nuclear layer (INL), the inner plexiform layer (IPL), and the retinal ganglion cell layer (RGCL). In contrast, in larvae derived from eggs injected with the *rtn4ip1* morpholino (MO; bottom), the structure of the retina is deeply disorganized, showing a total absence of the layers from the retinal ganglion cell layer to the outer plexiform layer. Scale bar represents 100 μm.

(C) The motility of zebrafish larvae was assessed with the touch response test at 72 hpf. The motion of individual larvae was monitored by a video camera after mechanical stimulation at the tail and was analyzed by the ImageJ software. Representative traces were obtained from the movies and the proportions of the different behaviors inferred from n = 9 for controls (Ctrl), n = 10 for MI morphant (MI), and n = 18 for the *rtn4ip1* morphant (MO).

Swimming behavior (left) showed normal longitudinal traces for the control larvae (Ctrl; top) (Movie S1) and the larvae issued from eggs injected with the mismatch morpholino (MI; middle) (Movie S2), whereas the majority of traces recorded for larvae derived from eggs injected with the *rtn4ip1* morpholino (MO; bottom) (Movie S3) were loopings. Quantification of the swimming behavior (right) from the three larvae types showed a normal mobility for the control and MI larvae, whereas *rtn4ip1*-silenced larvae showed motionless (25%) or looping (55%) behaviors, indicating possible paralysis and visual impairment, respectively.

impact on RGC dendritic growth and synaptogenesis and deleterious consequences on RGC survival, as reported in neurons and aging mice depleted for OPA1.[19,20] Our results also implicate RTN4IP1 in the response to UV light assaults,[21] a concept that is relevant to the neuroanatomical and physiological specificities of RGCs and that has been postulated to contribute to the selective vulnerability of these neurons in mitochondrial optic neuropathies.[11] Indeed, RGC soma are continuously exposed to exogenous short-wavelength light, which is known to modify mitochondrial function[22] and could therefore potentiate the deleterious effects of *RTN4IP1* mutations and further inhibit mitochondrial function sufficiently to compromise RGC survival. The identification of mutations in *RTN4IP1* in individuals with recessive optic neuropathy points toward a pathophysiological triad linking mitochondrial dysfunction, UV light susceptibility, and altered neuronal plasticity. Future work will in turn demonstrate whether these pathological interactions could be relevant to other optic neuropathies, including glaucoma.

Supplemental Data

Supplemental Data include three figures, one table, and three movies and can be found with this article online at http://dx.doi.org/10.1016/j.ajhg.2015.09.012.

Acknowledgments

Web Resources

The URLs for data presented herein are as follows:

ExAC Browser, http://exac.broadinstitute.org/
NHLBI Exome Sequencing Project (ESP) Exome Variant Server, http://evs.gs.washington.edu/EVS/
OMIM, http://www.omim.org/
PolyPhen-2, http://genetics.bwh.harvard.edu/pph2/
SIFT, http://sift.bii.a-star.edu.sg/

References

1. Lenaers, G., Hamel, C., Delettre, C., Amati-Bonneau, P., Procaccio, V., Bonneau, D., Reynier, P., and Milea, D. (2012). Dominant optic atrophy. Orphanet J. Rare Dis. 7, 46.

2. Maresca, A., la Morgia, C., Caporali, L., Valentino, M.L., and Carelli, V. (2013). The optic nerve: a "mito-window" on mitochondrial neurodegeneration. Mol. Cell. Neurosci. 55, 62–76.

3. Delettre, C., Lenaers, G., Griffoin, J.M., Gigarel, N., Lorenzo, C., Belenguer, P., Pelloquin, L., Grosgeorge, J., Turc-Carel, C., Perret, E., et al. (2000). Nuclear gene OPA1, encoding a mitochondrial dynamin-related protein, is mutated in dominant optic atrophy. Nat. Genet. 26, 207–210.

4. Ferré, M., Caignard, A., Milea, D., Leruez, S., Cassereau, J., Chevrollier, A., Amati-Bonneau, P., Verny, C., Bonneau, D., Procaccio, V., and Reynier, P. (2015). Improved locus-specific database for OPA1 mutations allows inclusion of advanced clinical data. Hum. Mutat. 36, 20–25.

5. Reynier, P., Amati-Bonneau, P., Verny, C., Olichon, A., Simard, G., Guichet, A., Bonnemains, C., Malecaze, F., Malinge, M.C., Pelletier, J.B., et al. (2004). OPA3 gene mutations responsible for autosomal dominant optic atrophy and cataract. J. Med. Genet. 41, e110.

6. Hanein, S., Perrault, I., Roche, O., Gerber, S., Khadom, N., Rio, M., Boddaert, N., Jean-Pierre, M., Brahimi, N., Serre, V., et al. (2009). TMEM126A, encoding a mitochondrial protein, is mutated in autosomal-recessive nonsyndromic optic atrophy. Am. J. Hum. Genet. 84, 493–498.

7. Metodiev, M.D., Gerber, S., Hubert, L., Delahodde, A., Chretien, D., Gérard, X., Amati-Bonneau, P., Giacomotto, M.C., Boddaert, N., Kaminska, A., et al. (2014). Mutations in the tricarboxylic acid cycle enzyme, aconitase 2, cause either isolated or syndromic optic neuropathy with encephalopathy and cerebellar atrophy. J. Med. Genet. 51, 834–838.

8. Hu, W.H., Hausmann, O.N., Yan, M.S., Walters, W.M., Wong, P.K., and Bethea, J.R. (2002). Identification and characterization of a novel Nogo-interacting mitochondrial protein (NIMP). J. Neurochem. 81, 36–45.

9. Fujii, M., Yasuda, K., Hartman, P.S., Ayusawa, D., and Ishii, N. (2011). A mutation in a mitochondrial dehydrogenase/reductase gene causes an increased sensitivity to oxidative stress and mitochondrial defects in the nematode Caenorhabditis elegans. Genes Cells 16, 1022–1034.

10. Ishi, N., Suzuki, N., Hartman, P.S., and Suzuki, K. (1993). The radiation-sensitive mutant rad-8 of Caenorhabditis elegans is hypersensitive to the effects of oxygen on aging and development. Mech. Ageing Dev. 68, 1–10.

11. Osborne, N.N., Li, G.Y., Ji, D., Mortiboys, H.J., and Jackson, S. (2008). Light affects mitochondria to cause apoptosis to cultured cells: possible relevance to ganglion cell death in certain optic neuropathies. J. Neurochem. 105, 2013–2028.

12. GrandPré, T., Nakamura, F., Vartanian, T., and Strittmatter, S.M. (2000). Identification of the Nogo inhibitor of axon regeneration as a Reticulon protein. Nature 403, 439–444.

13. Fournier, A.E., GrandPre, T., and Strittmatter, S.M. (2001). Identification of a receptor mediating Nogo-66 inhibition of axonal regeneration. Nature 409, 341–346.

14. Petrinovic, M.M., Duncan, C.S., Bourikas, D., Weinman, O., Montani, L., Schroeter, A., Maerki, D., Sommer, L., Stoeckli, E.T., and Schwab, M.E. (2010). Neuronal Nogo-A regulates neurite fasciculation, branching and extension in the developing nervous system. Development 137, 2539–2550.

15. Teng, F.Y., Ling, B.M., and Tang, B.L. (2004). Inter- and intracellular interactions of Nogo: new findings and hypothesis. J. Neurochem. 89, 801–806.

16. Huang, Y.Y., Tschopp, M., and Neuhauss, S.C. (2009). Illusionary self-motion perception in zebrafish. PLoS ONE 4, e6550.

17. Malicki, J., Neuhauss, S.C., Schier, A.F., Solnica-Krezel, L., Stemple, D.L., Stainier, D.Y., Abdelilah, S., Zwartkruis, F., Rangini, Z., and Driever, W. (1996). Mutations affecting development of the zebrafish retina. Development 123, 263–273.

18. Schmandke, A., Schmandke, A., and Schwab, M.E. (2014). Nogo-A: Multiple Roles in CNS Development, Maintenance, and Disease. Neuroscientist 20, 372–386.

19. Bertholet, A.M., Millet, A.M., Guillermin, O., Daloyau, M., Davezac, N., Miquel, M.C., and Belenguer, P. (2013). OPA1 loss of function affects in vitro neuronal maturation. Brain 136, 1518–1533.

20. Williams, P.A., Piechota, M., von Ruhland, C., Taylor, E., Morgan, J.E., and Votruba, M. (2012). Opa1 is essential for retinal ganglion cell synaptic architecture and connectivity. Brain 135, 493–505.

21. Birch-Machin, M.A., and Swalwell, H. (2010). How mitochondria record the effects of UV exposure and oxidative stress using human skin as a model tissue. Mutagenesis 25, 101–107.

22. del Olmo-Aguado, S., Manso, A.G., and Osborne, N.N. (2012). Light might directly affect retinal ganglion cell mitochondria

to potentially influence function. Photochem. Photobiol. *88*, 1346–1355.

23. Bénit, P., Slama, A., and Rustin, P. (2008). Decylubiquinol impedes mitochondrial respiratory chain complex I activity. Mol. Cell. Biochem. *314*, 45–50.

24. James, A.M., Wei, Y.H., Pang, C.Y., and Murphy, M.P. (1996). Altered mitochondrial function in fibroblasts containing MELAS or MERRF mitochondrial DNA mutations. Biochem. J. *318*, 401–407.

25. Rustin, P., Chretien, D., Bourgeron, T., Gérard, B., Rötig, A., Saudubray, J.M., and Munnich, A. (1994). Biochemical and molecular investigations in respiratory chain deficiencies. Clin. Chim. Acta *228*, 35–51.

26. Talmat-Amar, Y., Arribat, Y., Redt-Clouet, C., Feuillette, S., Bougé, A.L., Lecourtois, M., and Parmentier, M.L. (2011). Important neuronal toxicity of microtubule-bound Tau in vivo in Drosophila. Hum. Mol. Genet. *20*, 3738–3745.